Host porphobilinogen deaminase deficiency confers malaria resistance in *Plasmodium chabaudi* but not in *Plasmodium berghei* or *Plasmodium falciparum* during intraerythrocytic growth

Cilly Bernardette Schnider[a,b]#, Hao Yang[a], Lora Starrs[a], Anna Ehmann[a,*], Farid Rahimi[c], Elena Di Pierro[4], Giovanna Graziadei[d], Kathryn Matthews[e], Tania De Koning-Ward[e], Denis C. Bauer[f], Simon J. Foote[a], Gaetan Burgio[a]†§, Brendan J. McMorran[a]†§

[a] Department of Immunology and Infectious Disease, John Curtin School of Medical Research, The Australian National University, Canberra, ACT 2601, Australia.

[b] Department of Biomedical Sciences Faculty of Medicine and Health Sciences, Macquarie University, NSW 2109 Australia.

[c] Research School of Biology, The Australian National University, Canberra, ACT 2601, Australia.

[d] Fondazione IRCCS Ca' Granda - Ospedale Maggiore Policlinico, Rare Diseases Center, Internal Medicine Unit, Department of Medicine and Medical Specialties, Via Francesco Sforza, 35, 20122 Milan, Italy.

[e] School of Medicine, Deakin University, Warn Ponds, VIC 3216, Australia

[f] Health and Biosecurity, CSIRO, Sydney, NSW 2113, Australia.

Running Head: Malaria resistance in PBGD deficiency.

§ Denotes Senior and Corresponding authors.

Address correspondence to Brendan J. McMorran, brendan.mcmorran@anu.edu.au

or Gaetan Burgio, gaetan.burgio@anu.edu.au

Current address: Institute of Cell Biology, University of Bern, Bern, Switzerland.

*Current address: Mater Research Institute, University of Queensland, South Brisbane, QLD 4101, Australia

† Contributed equally to this work

Abstract word count: 280

Importance word count: 150

Main text word count (Introduction, Results, Discussion and Methods): 5,300

Number of figures/tables: four and two supplementary figures. Four supplementary tables.

ABSTRACT (280 words)

An important component in host resistance to malaria infection are inherited mutations that give rise to abnormalities and deficiencies in erythrocyte proteins and enzymes. Understanding how such mutations confer protection against the disease may be useful for developing new treatment strategies. A mouse ENU-induced mutagenesis screen for novel malaria resistance-conferring mutations identified a novel nonsense mutation in the gene encoding porphobilinogen deaminase (PBGD) in mice, denoted here as *Pbgd*^{MRI58155}. Heterozygote *Pbgd*^{MRI58155} mice exhibited approximately 50% reduction in cellular PBGD activity in both mature erythrocytes and reticulocytes, although enzyme activity was approximately 10 times higher in reticulocytes than erythrocytes. When challenged with blood-stage *P. chabaudi*, which preferentially infects erythrocytes, heterozygote mice showed a modest but significant resistance to infection, including reduced parasite growth. A series of assays conducted to investigate the mechanism of resistance indicated that mutant erythrocyte invasion by *P. chabaudi* was normal, but that following intraerythrocytic establishment a significantly greater proportions of parasites died and therefore affected their ability to propagate. The *Plasmodium* resistance phenotype was not recapitulated in *Pbgd*-deficient mice infected with *P. berghei*, which prefers reticulocytes, or when *P. falciparum* was cultured in erythrocytes from patients with acute

intermittent porphyria (AIP), which had modest (20-50%) reduced levels of PBGD. Furthermore, the growth of *Pbgd*-null *P. falciparum* and *Pbgd*-null *P. berghei* parasites, which grew at the same rate as their wild-type counterparts in normal cells, were not affected by the PBGD-deficient background of the AIP erythrocytes or *Pbgd*-deficient mice. Our results confirm the dispensability of parasite PBGD for *P. berghei* infection and intraerythrocytic growth of *P. falciparum*, but for the first time identify a requirement for host erythrocyte PBGD by *P. chabaudi* during *in vivo* blood stage infection.

IMPORTANCE (150 words)

The causative agent of malaria, *Plasmodium*, adopts a parasitic lifestyle during erythrocyte infection, and as such relies on host cell factors for its survival and growth. Host-encoded mutations that alter the availability of these factors confer disease resistance, including several well-known genetic erythrocyte abnormalities that have arisen due to the historical evolutionary pressure of malaria. This study identified in mice a novel malaria resistance-conferring host mutation in the heme biosynthesis enzyme, porphobilinogen deaminase (PBGD), and compared the relative requirements by *Plasmodium* for the host versus parasite-encoded forms of PBGD in both *in vivo* and *in vitro* settings. The findings demonstrated that parasite PBGD was dispensable, but that the host enzyme was important specifically during *in vivo* infection by *P. chabaudi*, and collectively suggest that *Plasmodium* requires a certain threshold of the enzyme to sustain its intraerythrocytic growth. *Plasmodium* may therefore be vulnerable to other interventions that limit host PBGD activity.

75 **INTRODUCTION**

76 Symptomatic and lethal stages of malaria occur when *Plasmodium* parasites invade and replicate
77 within erythrocytes. The ongoing relationship between parasite and host, spanning primordial
78 vertebrates and human evolutionary history, has exerted significant selective pressures on human
79 populations. This has manifested as polymorphisms and mutations that produce altered erythrocytic
80 proteins, many of which are associated with host resistance to infection. These include
81 hemoglobinopathies, and deficiencies in cytoskeletal proteins and various enzymes that are highly
82 expressed in erythrocytes; they act either directly by impeding parasite invasion or growth, or
83 indirectly on host immune responses and parasite clearance [1; 2; 3; 4]. By virtue of its parasitic
84 lifestyle during the blood-stage of the disease, *Plasmodium* also scavenges erythrocyte enzymes,
85 including protein kinases, cellular redox regulators, and those involved in heme biosynthesis [5; 6; 7;
86 8; 9]. Depriving parasites of such host enzymes may contribute to resistance to *Plasmodium* infection
87 and facilitate identifying novel antimalarial therapeutics as reported in model systems [10; 11].

88 Heme is an essential cofactor in many proteins and enzymes, for example in hemoglobin as the carrier
89 of oxygen. The canonical heme biosynthetic pathway uses eight enzymes, which catalyze conversion
90 of glycine and succinyl-CoA into protoporphyrin, and subsequent Fe^{2+} incorporation. Heme
91 biosynthesis is essential in humans and complete deficiency of any of the synthetic enzymes is lethal.
92 However, mutations that reduce enzyme production or activity are known and cause porphyria.
93 Characteristic symptoms of porphyria may include mild to severe skin photosensitivity, liver
94 malfunction and neurological problems, and are caused by build-up of toxic porphyrin precursors and
95 their derivatives. Specific symptoms and disease severity depend on the composition and levels of
96 these molecules, which in turn are determined by enzyme activity and responsible mutations.

97 *Plasmodium* has a canonical heme biosynthesis pathway [12]. Interestingly, essentiality of the
98 pathway differs depending on the parasite life-cycle stage. *P. berghei* made genetically deficient in
99 either the first (δ-aminolevulinic acid synthase; ALAS) or last (ferrochelatase; FC) enzyme of the

100 pathway are not viable in the mosquito stages, but propagate in the mouse bloodstream and cause
101 symptoms that are indistinguishable from those by wild-type parasites [12; 13]. Another study in *P.*
102 *berghei* has reported a similar requirement for porphobilinogen deaminase (PBGD) in mosquito but
103 not erythrocyte stages of growth [14]. Similarly, *P. falciparum* carrying deletions in FC, PBGD or
104 another pathway enzyme, coproporphyrinogen oxidase grow normally when cultured in human
105 erythrocytes [12; 15].
106 How these enzyme-deficient parasite lines obtain heme is topic of some controversy. Based on the
107 observation that no heme was synthesized in an FC-deficient *P. falciparum* [12], acquisition directly
108 from the degradation of host hemoglobin was suggested a likely source [12]. However, co-opting of
109 the host heme-biosynthetic enzymes to participate in *de novo* synthesis has been demonstrated in
110 other studies [5; 9; 16]. Notably, although heme biosynthesis is restricted to erythroid progenitors,
111 mature erythrocytes contain detectable amounts of active enzymes [17; 18; 19] including PBGD,
112 which is biosynthetically active in reticulocytes and mature erythrocytes [15; 20].
113 Previously, we showed that the growth of both *P. chabaudi* and *P. falciparum* was significantly
114 perturbed in mouse and human erythrocytes with reduced levels of FC (erythropoietic protoporphyric
115 erythrocytes). In contrast, *P. falciparum* grew normally in X-linked dominant protoporphyric
116 erythrocytes, which have normal levels of FC, but elevated porphyrin precursors [21]. In addition,
117 treatment with FC substrate analogues that specifically inhibit the enzyme killed cultured blood stage
118 *P. falciparum*, and inclusion of excess enzyme substrate rescued the effect [11; 21]. Collectively, this
119 indicated that *Plasmodium* has a specific requirement for host FC to sustain its intraerythrocytic
120 growth in erythrocytes. Here we identified a novel mutation in the gene encoding PBGD in mice that
121 reduced erythrocytic enzyme activity and compared the growth requirements of *Plasmodium* for host
122 versus parasite-encoded PBGD in both *in vitro* and *in vivo* settings of blood stage infection.
123
124

125 **RESULTS**

126 In a large-scale ENU mutagenesis screen for abnormal red blood cell count, we discovered a mouse,
127 denoted as MRI58155, which displayed microcytosis accompanied by moderately elevated
128 reticulocyte counts, reduced hematocrit and total hemoglobin, but with normal mean erythrocytic
129 hemoglobin levels. We confirmed that the phenotype was heritable after crossing the MRI58155 G1
130 animal with SJL/J mice and observing that the G1 microcytosis phenotype was passed on to
131 approximately half the offspring. Intercrossing two affected G2 mice produced the wild-type
132 phenotype in approximately one third of the progeny and the G1 founder phenotype in the other two
133 thirds (Table S1). Collectively this indicated a fully penetrant dominant inheritance of the
134 microcytotic phenotype (i.e., heterozygous for the MRI58155 allele), but embryonic lethality in
135 homozygotes.

136 Whole-exome sequencing of two heterozygous G3 mice and subsequent segregation analysis of
137 mutations in candidate genes identified a single base substitution (A to G) in chromosome 9 (Chr9
138 nucleotide position 44341074, mm10), which is located in the murine *Pbgd* gene (NM_013551). This
139 mutation designated $Pbgd^{MRI58155}$ is predicted to disrupt splicing of exon 6 and result in a truncated
140 protein comprising 90 amino acids; this theoretical protein lacks all conserved residues and domains
141 required for catalytic function of PBGD (Figure 1A). The mutation completely segregated with the
142 microcytic phenotype over more than 10 generations of breeding, excluding the possibility that other
143 mutations were involved in the phenotype. No detectable differences in PBGD protein levels were
144 seen in extracts from spleen, liver, bone marrow, or erythrocytes from heterozygous versus wild-type
145 mice and the predicted 20 KD truncated was not observed (data not shown). However, PBGD enzyme
146 activity, measured using a specific and sensitive assay, was approximately 50% lower in
147 heterozygous versus wild-type purified mature erythrocytes (3.38 ± 1.80 versus 6.53 ± 2.14 nkat/L;
148 p = 0.048) (Figure 1B). We also separately purified and assayed PBGD activity in reticulocytes.
149 Activity in the mutant reticulocytes was also relatively lower than in wild-type reticulocytes (22.1 ±

150 14.3 versus 60.0 ± 36.3 nkat/L; $p = 0.08$) (Figure 1B), although, notably, the reticulocyte values were
151 approximately 10 times higher than respective erythrocyte values. Urine from heterozygous mice
152 appeared slightly pink, indicative of excretion of excess porphoryrin synthetic precursors. The
153 heterozygous mice also exhibited a modest splenomegaly, but normal liver size and normal iron
154 content in both organs; serum cytokine levels were also similar to those in wild-type mice (Tables S2
155 and S3). Erythrocyte life span (Figure S1A) and osmotic fragility (Figure S1B) were also unaffected
156 by the mutation. In addition, production of erythroid progenitors was unaffected (Figure S1C). No
157 homozygous animals were generated from intercrossing more than different 10 pairs of *Pbgd*^{MRI58155}
158 heterozygotes, indicating the homozygous *Pbgd*^{MRI58155} mutation was probably embryonic lethal.
159
160 To investigate if the *Pbgd*^{MRI58155} mutation affects the host resistance to malarial infection, cohorts of
161 heterozygous and wild-type mice were inoculated with blood stage *P. chabaudi adami* DS, which is
162 typically lethal to this parental mouse strain (SJL/J). We observed an altered course of infection in
163 heterozygotes compared to wild-types. Parasitemias were significantly lower in the heterozygotes
164 between days seven and ten in female mice (Figure 2A), and days nine and ten in male mice (Figure
165 2B). A modest but highly significant survival advantage was also observed for female heterozygotes
166 ($p = 0.0016$); 90% of these animals survived for at least one day longer than their wild-type
167 littermates, although 12 of 13 heterozygous mice eventually succumbed (Figure 2C). Two of 21
168 heterozygous male mice survived the infection, but this was not statistically significant (Figure 2D).
169 We investigated whether the reduced parasitemia observed in the heterozygous mice was due to
170 compromised merozoite invasion of erythrocytes. To assess this we used an *in vivo* erythrocyte-
171 tracking assay (IVET) [22], where a mixture of heterozygous and wild-type erythrocytes, each
172 labelled with a different fluorescent dye, was transfused into recipient wild-type mice infected with
173 *P. chabaudi* (at the point of parasite schizogony), and the relative proportions of donor cells that
174 became infected were determined over time. There were no differences between the proportions

175 infected heterozygous and wild-type cells measured between 30 min and 20 h after cell transfer. After
176 39 h the parasitemia increased relative to the earlier timepoints, reflecting a second schizogony and
177 infection cycle, but there were still no apparent differences between the donor cells (Figure 2E). These
178 results indicate that the *P. chabaudi* merozoites invade *Pbgd*^{MRI58155} heterozygous and wild-type
179 erythrocytes at similar rates. We also investigated if *P. chabaudi* intraerythrocytic growth was
180 impaired by PBGD insufficiency. Dead or dying intraerythrocytic *P. chabaudi* were identified using
181 an adapted terminal deoxynucleotidyl transferase dUTP nick end labeling (TUNEL) assay [23]. The
182 mean percentages (± SEM) of TUNEL-labeled parasites measured in mouse blood samples collected
183 eight and nine days after *P. chabaudi* infection were 9.0 ± 1.0 and 12.6 ± 1.2 in wild-type mice and
184 10.4 ± 1.4 and 15.8 ± 1.7 in heterozygous mice; the heterozygous values were significantly greater
185 than those of the wild-type mice at both time points (p <0.05; Figure 2F). This finding suggests that
186 in heterozygous erythrocytes, a greater proportion of parasites were dying, which in turn may reduce
187 production of new, viable parasites and thereby provides an explanation for the observed reduction
188 in parasitemia and improved survival.
189 The *Pbgd*^{MRI58155} heterozygous mice were also challenged with another murine malarial parasite, *P.*
190 *berghei* ANKA (Pb ANKA), which preferentially infects reticulocytes and in the SJL/J mouse strain
191 causes severe anemia without any cerebral malaria symptoms. We also generated a *P. berghei* parasite
192 line in which the parasite *Pbgd* (PbA_060800) was deleted (PbA_Pbgd, Figure S2). There were no
193 differences in the parasite growth rates between the heterozygous and wild-type mice infected with
194 wild-type parasites, and the *Pbgd* knockout and wild-type parasites propagated equivalently in both
195 mouse strains (Figure 3). There were also no differences in the disease course or susceptibility over
196 the period of the infection (17 days); mice were ethically euthanized after this time. Collectively these
197 data indicate that the *Pbgd*^{MRI58155} mutation conferred resistance to *P. chabaudi* infection but not *P.*
198 *berghei* infection, and that the parasite-encoded PBGD was dispensable for *P. berghei* infection
199 irrespective of the host PBGD sufficiency status.

200 PBGD deficiency in humans can manifest as AIP (MIM 176000). AIP is characterized by occasional,
201 acute episodes of gastrointestinal and neuropathic symptoms; between episodes, the patient is healthy.
202 Acute attacks result in high urinary excretion of the heme precursors, especially δ-aminolevulinic
203 acid and porphobilinogen [24]. We obtained blood samples from four AIP patients (A – D), all with
204 the same confirmed *PBGD* gene mutation (PBGD c.[913 G>C];[=]). This mutation has not been
205 reported previously. It is predicted to cause a splice site mutation and premature termination of
206 translation, resulting in a carboxyl-terminal deletion (His305-Ter362) and an inactive protein. PBGD
207 enzyme activity levels measured in whole blood samples from these patients were between 50 and
208 80% of normal levels (Table S4). All of the patients reported a typical history of episodes of acute
209 symptoms with elevated urinary δ-aminolevulinic acid and porphobilinogen levels, and two were
210 symptomatic at the time of blood collection.
211 Isolated erythrocytes from these AIP patients as well as two healthy individuals, one collected in Italy
212 (Normal Italy) and one from an Australian Red Cross Blood Service red cell donor (Normal ARC),
213 were infected with growth-stage-synchronized *P. falciparum* (pigmented trophozoites and schizonts).
214 Cultures were incubated for up to 72 h and sampled at different time points to count the number of
215 parasitized cells and compare parasite propagation over time. Following the first 24 h of culturing,
216 after parasites had egressed from donor erythrocytes and invaded the surrounding test cells, we
217 observed no differences in parasitemia fold-change between the AIP and healthy control cells. After
218 48 h, parasites had developed from early ring stage into mature trophozoite and schizont forms of the
219 parasite, and similar proportions were observed between the AIP and control cells. After 72 h,
220 parasites had replicated in the test erythrocytes and undergone a further cycle of schizogony and cell
221 invasion; the parasitemia fold changes in all of the control and AIP samples were also similar at this
222 time point (Figure 4). In the same experiments we also infected these control and AIP cells with a *P.*
223 *falciparum* clone carrying a genetic disruption of the parasite *Pbgd* homolog (PF3D7_1209600); this
224 was shown previously to grow as well as its wild-type parent strain (3D7) in normal human

225 erythrocytes [15]. The *Pbgd* deleted line grew similarly to the wild-type line in all of the erythrocyte
226 samples, and no differences in parasitemia fold change were observed after 24 or 72 h of culture
227 (Figure 4). Collectively, these results indicated that neither the invasion or intraerythrocytic growth
228 of both wild-type and *Pbgd* deleted *P. falciparum* were sensitive to the AIP host cell PBGD
229 insufficiency.
230

231 **DISCUSSION**

232 Here we investigated if malarial parasites require the heme biosynthetic enzyme PBGD for
233 intraerythrocytic growth and infection. This idea was motivated by previous observations that other
234 host heme biosynthetic enzymes as well as precursors of the pathway are co-opted by the parasite [5;
235 9; 11; 16; 21]. To do this, we used a combination of genetic models of PBGD insufficiency and
236 deficiency in mouse, human and *Plasmodium* to compare and contrast parasite growth and the
237 mechanisms of host resistance to malarial infection.
238 In mice, PBGD insufficiency was generated through the identification and characterization of a novel
239 ENU-induced mutation in the murine *Pbgd* gene ($Pbgd^{MRI58155}$). Mice heterozygous for this mutation
240 displayed a relatively normal phenotype, distinguished by microcytosis and a modest, but significant
241 decrease in PBGD activity, although they exhibited no overt symptoms characteristic of AIP.
242 Previous studies have shown that a profound deficiency of PBGD in mice is necessary to mimic
243 human AIP [25]. The protein expressed by the $Pbgd^{MRI58155}$ allele is predicted to be truncated and
244 completely inactive. Consistent with this prediction, we never obtained homozygous pups and
245 demonstrated approximate 50% reductions PBGD enzyme activity in both mature reticulocyte-
246 depleted erythrocytes and in purified reticulocytes. The most prominent consequence of the
247 $Pbgd^{MRI58155}$ mutation, and indeed the phenotypic basis of its identity, was a modest microcytic
248 anemia, although erythrocyte number and erythrocytic hemoglobin concentrations were normal.
249 Reduced biosynthesis of heme in erythroid progenitors can often lead to generation of microcytic

250 anemia, although this is not characteristic of human AIP, and is not a reported effect in mouse lines
251 with the *Pbgd*-null or hypomorphic mutations [25]. However, microcytic erythrocytes have been
252 observed in cats with *Pbgd* mutations displaying AIP symptoms [26]. Overall, the $Pbgd^{MRI58155}$ allele
253 results in a phenotype consistent with a mild, asymptomatic form of AIP.
254 We found that the propagation of the murine malarial parasite *P. chabaudi* was reduced in the
255 $Pbgd^{MRI58155}$ heterozygous mice and survival to infection was improved. Our data suggests the most
256 likely reason for the resistance is the compromised ability of *P. chabaudi* to survive within the mutant
257 erythrocytes. We specifically excluded other possible explanations for the resistance, including
258 merozoite invasion, immune responses, iron status and erythrocyte structure and function. However,
259 another murine-specific species *P. berghei* grew normally in the $Pbgd^{MRI58155}$ mice, as did *P.*
260 *falciparum* cultured in human AIP (PBGD-insufficient) erythrocytes. The growth and infectivity of
261 *P. falciparum* and *P. berghei* were also compared with genetically modified lines in which the
262 respective parasite *Pbgd* loci were deleted (including a new *Pbgd*-null *P. berghei* line generated in
263 this study). Each *Pbgd*-deleted species grew as well as their wild-type counterpart when introduced
264 into the normal and AIP erythrocytes, or the wild-type and $Pbgd^{MRI58155}$ mice, respectively.
265 Collectively, these results suggest that parasite PBGD is completely dispensable for blood stage
266 growth of *P. falciparum* and *P. berghei*, confirming previous studies [14; 15] and, at least under the
267 conditions used here to grow the parasites, that host erythrocyte PBGD is also not important. In order
268 to understand why *P. chabaudi* but not *P. berghei* exhibits reduced growth in the $Pbgd^{MRI58155}$ mouse,
269 an important distinction is the approximate 10-fold lower PBGD activity measured in the erythrocytes
270 versus reticulocytes. *P. chabaudi* and *P. berghei* have respective tropisms for these cells, so the
271 former must survive in a lower PBGD environment and may therefore be more sensitive to the added
272 scarcity of PBGD in the mutant cells. In other words, the parasite may require a certain threshold
273 level of host PBGD to efficiently develop and propagate within the erythrocyte. It is also possible
274 that the mutation has other indirect effects on *P. chabaudi* but not *P. berghei* or that these species

275 have differences in their acquisition or requirement for heme. The relatively mild decreased PBGD
276 activities in the AIP erythrocytes may be insufficient to affect *P. falciparum* (also an erythrocyte-
277 preferring species) under culture conditions.
278 In conclusion, our data suggest that erythrocyte-stage *Plasmodium* is sensitive to profound but not
279 mild deficiencies in erythrocyte PBGD enzyme activity and speculate other strategies that acutely
280 reduce or temporally block PBGD could be effective at preventing parasite growth.
281
282
283
284 **METHODS**
285 **Ethics statement**
286 Blood sampling and experimental procedures involving patients were performed in accordance with
287 the 1983 revision of the Declaration of Helsinki. The study was approved by the Ethical Committee
288 of Fondazione IRCCS Ca' Granda, Ospedale Maggiore Policlinico, Milan, Italy (Project Number
289 246_2015) and The Australian National University Human Research Ethics Committee (2014/765).
290 Written informed consent was obtained for each subject prior to study participation.
291 All procedures involving animals conformed to the *Australian code of practice for the care and use*
292 *of animals for scientific purposes* guidelines by the Australian National Health and Medical Research
293 Council and were approved by Macquarie University Animal Ethics Committee (Project Numbers:
294 ARA 2012/017 and 2012/019), the Australian National University Animal Experimentation Ethics
295 Committee (2014/53) and Deakin University animal ethics committee (Project Number G37-2013).
296
297
298 **Animals**

299 Mice were bred and housed under specific pathogen-free conditions. Mice were housed under
300 controlled temperature (21°C) with a 12:12 h light–dark cycle and fed a diet of Rat and Mouse
301 Premium Breeder chow (Gordons Specialty Feeds, Glen Forest, WA, Australia). Seven-week-old
302 SJL/J male mice were injected intraperitoneally (IP) with 150 mg/kg of *N*-ethyl-*N*-nitrosourea (ENU)
303 three times at one-week intervals. Mutagenized G0 mice were crossed with background SJL/J mice.
304 G1s were bled after seven weeks for blood analysis. The G1 58155 founder displayed a mean
305 corpuscular volume that was two standard deviations smaller than average for the colony; it was
306 crossed with SJL/J and resulting G2s were used in further experiments. For each experimental
307 procedure, heterozygous $Pbgd^{MRI58155}$ mice were compared to their wild-type littermates and housed
308 together, up to five animals per cage (Green Line IVC, Tecniplast, PA). Sample sizes were chosen
309 based on statistical power calculations to limit the number of animals used. For generating *P. berghei*
310 *Pbgd*-knockout parasites, 6-8 week-old BALB/c mice were used.
311
312 **Mouse phenotyping**
313 Complete blood cell counts were obtained using an ADVIA® 2120 hematology system. Erythroid
314 progenitors were examined by staining the bone-marrow-derived cells from mutant and wild-type
315 mice with anti-TER119 and anti-CD44 (eBioscience). Cells were analyzed on a BD FACSARIA™-
316 II flow cytometer, recording 10,000 events per sample. Populations were gated as described [27].
317 Cytokine Flexset assays (BD Bioscience) were used to measure plasma cytokine concentrations
318 according to the manufacturer's instructions.
319 Erythrocyte life span was determined by following intravenous administration of 1 mg of NHS-
320 biotin-ester dissolved in 0.9% (w/v) saline, and blood sampling by tail-snipping each day for seven
321 days, and staining with anti-TER119 and anti-CD71 (eBioscience). Cells were suspended in
322 phosphate-buffered saline (PBS; 10 mM sodium phosphate, 2.7 mM KCl, 140 mM NaCl, pH 7.4)

323 containing 1% (w/v) BSA solution containing 10^8 counting beads/μL, and the number of $TER119^+$
324 $CD71^-$ cells calculated per bead.
325 Hepatic and splenic iron levels were measured in tissues dried at 45 °C for 48 h and then digested in
326 a 10% hydrochloric acid/10% trichloroacetic acid (TCA) solution for 48 h at 65 °C, and values
327 normalized according to tissue dry weight. Samples were centrifuged (10000×*g* for 5 min); 200 μL
328 of supernatant was added to 1 mL of 1,10-phenanthroline monohydrate solution and incubated for 15
329 min at ~23 °C. After incubation, absorbance was measured at λ = 508 nm.
330 Erythrocytic osmotic fragility was determined by incubating blood samples diluted 1:100 in NaCl
331 solutions ranging from 0 to 160 mM. After 30 min at 37 °C, samples were centrifuged and absorbance
332 of the supernatant measured at λ = 545 nm. Percentage lysis was calculated by comparison to 100%
333 lysis in pure water.
334
335 **Whole-exome sequencing**
336 DNA from two MRI58155 mice was isolated using a Qiagen DNeasy Blood and Tissue Kit (Hilden,
337 Germany). DNA (≥10 μg) was prepared for paired-end genomic library sequencing using a kit from
338 Illumina (San Diego, CA). Exomes were enriched using the Agilent SureSelect kit. Samples were
339 sequenced using a Hiseq 2000 platform. Variants were identified and filtered as described [28].
340 Briefly, we mapped the short sequence tags (reads) on the mouse genome (mm10/NCBI38) using
341 BWA V0.61 [29] and BOWTIE2 [30]. Nucleotide variants were identified using SAMTOOLS
342 V0.1.19 [31] and GATK [32]. Through our variant-filtration process, we retained those variants that
343 are "common" and "private" to the two sequenced animals, and not shared by other SJL/J mice. These
344 variants were annotated using ANNOVAR [33].
345
346 **PBGD assay**

347 Purified erythrocytes and reticulocytes were prepared for assaying PBGD activity as follows. Whole
348 blood was collected by cardiac bleeding, mixed with anticoagulant (1/10 volume 85 mM sodium
349 citrate, 69 mM citrate and 111 mM glucose), immediately centrifuged at 150×*g* for 10 min, and the
350 plasma and buffy coat removed. The retained red cells were then centrifuged through 75% Percoll
351 PBS-buffered solution (800×*g* for 10 min) to remove residual leukocytes. Erythrocytes were depleted
352 of reticulocytes (and the reticulocytes separately retained) by addition of allophycocyanin (APC)-
353 conjugated rat anti-mouse CD71 antibodies (1 µg/mL; clone RI7 217.1.4; eBioscience™) followed
354 by MojoSort™ Mouse anti-APC Nanobeads (1/10 volume; Biolegend®) and magnetic affinity
355 separation using a QuadroMACS™ Separator (Miltenyi Biotec). The resulting erythrocyte
356 preparations were confirmed to be free of reticulocytes using flow cytometry (>99.9% pure).
357 Erythrocytes and reticulocytes were assayed for PBGD by incubating 2 µL cells diluted 50-fold in
358 the assay buffer (50 mM Tris containing 0.2% Triton X-100, 20 mM citric acid, pH 8.2), incubated
359 at 56 °C for 15 min, and finally cooled on ice. Duplicate aliquots (40 µL) of the resulting hemolysates
360 were mixed with 80 µL assay buffer containing 80 µM porphobilinogen (Sigma Aldrich, Castle Hill,
361 Australia) and incubated at 37 °C for 60 min to permit the PBGD-catalyzed generation of
362 hydroxymethylbilane. The reaction was terminated by adding 120 µL 12.5% TCA and incubated for
363 30 min at ~23 °C, which results in the non-enzymatic conversion (oxidation) of hydroxymethylbilane
364 to uroporphyrinogen I (URO I). After centrifugation (1000×*g*, 5 min), 150 µL of clarified supernatant
365 was transferred to brown glass vials, stored at 4 °C, and subjected to ultrahigh-performance liquid
366 chromatography (UHPLC) within 72 h to quantify URO I levels. Samples (100 µL) were injected
367 and analyzed in a UHPLC system consisting of a Dionex UltiMate™ 3000 in line with a fluorescence
368 FLD-3400 detector. A Hypersil Gold C18 column (1.9 µm particle size, 50 × 2.1 mm internal
369 diameter; Thermo Fisher Scientific, Australia) was used for elution. The mobile phase consisted of
370 9% (v/v) acetonitrile in 1 M ammonium acetate–acetic acid buffer, pH 5.16 (solvent A), and 10%
371 acetonitrile (v/v) in methanol (solvent B) [34; 35; 36]. The elution program was 0% B (100% A) for

372 initial 2 min, 0% B (100% A) to 10% B (90% A) for 2–6 min, 10% B (90% A) to 90% B (10% A)
373 for 1 min, and isocratic 90% B for further 2 min. The flow rate was set at 0.8 mL/min and column
374 temperature at 35 °C. Eluents were detected at λ_{ex} = 404 nm and λ_{em} = 618 nm. To quantify standards,
375 a solution containing 400 nmol/L URO I in 12.5% TCA was prepared using a 1 mM stock solution
376 dissolved in 1 M HCl (Sigma Aldrich). The concentration of the standard was calculated using
377 absorbance at λ = 405 nm and $\varepsilon = 505 \times 10^3$ L cm^{-1} mol^{-1} [36]. Standard curves were generated by
378 varying the injection volume and integrating the corresponding peaks. Enzyme activity was
379 calculated as nkat/L cells according to Erlandsen et al 2000 [29].
380
381 ***P. falciparum* culture**
382 *P. falciparum* was cultured in O^+ human erythrocytes at 2.5% hematocrit according to a previously
383 described method [37]. The cell-culture medium (CCM) comprised of RPMI 1640 supplemented with
384 8.8 mM D-glucose, 22 mM HEPES, 208 nM hypoxanthine (Sigma-Aldrich, Missouri, US), 46.1 nM
385 gentamicin, 2.1 g/L AlbuMAX® I, 2.8 mM L-glutamine (Life Technologies, Australia), and 4.2%
386 (v/v) O^+ human serum. Cultures were maintained in flasks filled with 1%O_2/3%CO_2/96%N_2 gas mix,
387 and kept in an orbitally shaking incubator at 50 rpm at 37°C. Culture parasitemias were maintained
388 at between 0.5% and 10%, and checked every one to two days by visualizing Giemsa-stained thin
389 blood smear by microscopy. CCM was changed every one to two days by pelleting infected cells at
390 500x*g* for 5 minutes and suspending them in fresh CCM. Human erythrocytes and sera were provided
391 by the Australian Red Cross Blood Service. Blood was washed thrice using CCM that lacked
392 hypoxanthine, AlbuMAX® I, and human serum, and centrifuged at 2800 RPM for 5 minutes after
393 each wash. The *P. falciparum* strain 3D7 was donated by Robin F. Anders (La Trobe University,
394 Melbourne, Australia). The Pf*Pbgd*-KO and 3D7 wild-type parental lines were gifts from Daniel E.
395 Goldberg (Washington University School of Medicine, St. Louis, MO).
396

397 **TUNEL staining and immunofluorescence**

398 Deoxyuridine triphosphate nick-end labeling by the terminal deoxynucleotidyl transferase (TUNEL)
399 labels degraded or sheared DNA, revealing apoptosis or necrosis. TUNEL and cell staining for
400 immunofluorescence microscopy were performed on blood smears from mice infected with *P.*
401 *chabaudi* infected mice as described [23], but with some modifications. Mouse blood samples were
402 fixed for at least 24 h in Cytofix solution (BD Biosciences) diluted fourfold in PBS. Slides coated
403 with polyethylenimine (0.1% v/v in PBS) were smeared with fixed blood and stained overnight in the
404 reaction mix from the Apo BrdU TUNEL Assay Kit (Molecular Probes, Eugene, OR). TUNEL-
405 labeled DNA was detected using a biotinylated anti-BrdU antibody and streptavidin-Alexa Fluor 594
406 conjugate (ThermoFisher Scientific, Australia). At least 100 infected cells were counted on each slide.
407 After staining, slides were mounted in SlowFade™ Gold Antifade Mountant with DAPI
408 (ThermoFisher Scientific, Australia) and glass coverslips (#1 from Menzel-Gläser). Slides were
409 examined at room temperature using an inverted Axio Observer fluorescence microscope or a LSM
410 800 confocal microscope with Airyscan, both using 630× magnification and coupled to a Axiocam
411 503 monochrome cameras (Zeiss, Australia). All acquired images were acquired and processed by
412 using the Zeiss Zen lite microscope software (Zeiss, Australia).

413

414 **Generation of *P. berghei pbgd* knockout.**

415 The *P. berghei ANKA pbgd* locus (*PbA_pbgd*, PBANKA_0608000) was targeted as follows. A
416 targeting plasmid, p35/EF5′.K$^+$GFP.CAM3′ was modified [40] by replacing the K$^+$GFP sequence
417 with firefly luciferase, yielding the vector p35/EF5′.FF.CAM3′. The 500 bp 5′ flanking sequence of
418 *PbA_pbgd* was amplified by PCR using the primers PbA_060800/5′FIF (5′-
419 gacccgcggGATCATTATGGCAAATATTCTGCC) and PbA_060800/5′FIR (5′
420 gacctgcagTATTGCTATAACTATATTATTCAGTTA), digested with *Sac*II and *Pst*I enzymes and
421 cloned into the corresponding sites of p35/EF5′.FF.CAM3′ to generate p35/5'Fl/EF5′.FF.CAM3′.

422 For the 3' homology arm, the 3′ flanking sequence of *PbA_pbgd* was amplified by PCR using the
423 primers PbA_060800/3′FIF (5′-gacgatatcGGATGAGGCAGCTTTATATTACA) and
424 PbA_060800/3′FIR (5′gacgaattcGTTCAAATCGCGTATTTGAATGTGATGTG), digested with
425 *Eco*RV and *Eco*RI and cloned into the corresponding sites of p35/5'Fl/EF5′.FF.CAM3′ to generate
426 p35/5+3'Fl/EF5′.FF.CAM3′. The plasmid vector was then linearized with *Sac*II/*Eco*RI and
427 transfected into PbANKA parasites using previously established methods [41]. The transfected
428 parasites were inoculated into a BALB/c naïve mouse by intravenous inoculation and selected for by
429 administering pyrimethamine into the mouse's drinking water (0.07 mg/mL) for six days. Parasite
430 DNA was extracted and a PCR was conducted to check for successful integration using the following
431 primers PbA_060800_int_F (primer 539, 5′-ATCCGAGCAATATTATCGACAG), hDHFR_R_int
432 (primer 540, 5′-GATGCAGTTTAGCGA-ACCAAC), CAM3'_F_int (primer 541, 5′-
433 GTAAAGGGTTAATTCTTATATGGTC) and Pb060800_int_R (primer 542, 5′-
434 CCATTTTCTCAATACTTACATAG) (Figure S2). The *PbA_pbgd* parasite was single cloned into
435 6-8 weeks old BALB/c mice by limiting dilution and verified by PCR according to the procedure
436 described previously [42].
437
438
439 ***P. chabaudi* and *P.berghei* infections**
440 Infection experiments used the rodent parasite *P. chabaudi adami* DS (408XZ) and *P. berghei*
441 ANKA. Parasite stocks were prepared by passage through resistant C57BL/6 (*P. chabaudi*) or
442 BALB/c (*P. berghei*) mice as described previously [22]. Experimental mice were infected by IP
443 injection with a dose of 1×10^4 parasitized erythrocytes. Blood-stage parasitemia was determined by
444 microscopically examining thin blood smears obtained by tail bleeding (1 μL per day from days seven
445 to 14 after infection) and staining with 10% Giemsa solution. Percentages of infected erythrocytes
446 were calculated from a minimum of 1,000 erythrocytes counted.

447

448 **Study subjects**

449 We studied erythrocytes obtained from four Italian Caucasian AIP patients recruited at the
450 Department of General Medicine, Fondazione IRCC Ca' Granda, Ospedale Maggiore Policlinico,
451 Milan, Italy. All patients had a confirmed biochemical and genetic diagnosis: two patients were
452 asymptomatic carriers and two experienced typical acute attacks. The biochemical measures
453 associated with the condition are provided in Table S4.

454

455 **Collection and preparation of purified erythrocytes**

456 Blood from four patients with AIP and the Italian healthy control subject was collected by
457 venepuncture into 5-mL tubes containing EDTA. These five blood samples were stored at 4°C and
458 shipped together within seven days of collection from the Ospedale Maggiore Policlinico, Milan,
459 Italy to The Australian National University (ANU), Canberra, Australia. Erythrocytes were purified
460 at the ANU by centrifugation (170×*g*, 13 min) to separate them from the plasma and white-cell
461 fractions. The erythrocytes were removed and washed twice in RPMI before being infected with
462 parasites.

463

464 ***P. falciparum* growth-inhibition assays**

465 For growth assays, parasites were propagated in normal erythrocytes (from the Australian Red Cross
466 Blood Service), purified using Percoll density-gradient centrifugation [38], and then added to test
467 erythrocytes at a final parasitemia of ~1%. Parasitemias were determined in samples collected during
468 culturing for up to 72 h. Samples were fixed in Cytofix solution (BD Biosciences) for 24 h, and then
469 washed once in PBS and stained with 5 μg/mL Hoechst 33342 for 5 min. Fluorescence signals were
470 measured using an LSR Fortessa cell analyzer (BD Biosciences). At least 100,000 events were
471 recorded per sample. BD FACS software was used to process and analyze the data.

Statistical analysis

For malaria survival, statistical significance was determined using the Mantel–Cox test. For other results, two-tailed Students *t*-test or ANOVA were used as indicated. A *p*-value of < 0.05 was considered significant.

ACKNOWLEDGMENTS:

The Authors were supported by an International Macquarie University Research Excellence Scholarship (CBS), the NHMRC (490037, 605524, APP1047090 and APP1066502), the Australian Research Council (DP120100061) and the National Collaborative Research Infrastructure (NCRIS) via the Australian Phenomics Network (APN). Funders had no role in the design of the study and collection, analysis, and interpretation of data or in writing the manuscript. We thank Ceri Flowers for administrative support, Diana Spinelli for recruitment of the AIP patients, Shelley Lampkin for technical assistance, Elinor Hortle for assisting with the cytokine assays, Gavin Symonds and Zeiss Australia for confocal imaging analysis, and the Australian Red Cross Blood Service for red cells and human serum.

496 **Author Information:**

497

498 Department of Immunology and Infectious Disease, John Curtin School of Medical Research, The
499 Australian National University, Canberra, ACT 2601, Australia.
500 Cilly Bernardette Schnider, Hao Yang, Lora Starrs, Anna Ehmann, Simon J. Foote, Brendan J.
501 McMorran, Gaetan Burgio

502

503 Department of Biomedical Sciences Faculty of Medicine and Health Sciences, Macquarie University,
504 NSW 2109 Australia.
505 Cilly Bernardette Schnider
506 Research School of Biology, The Australian National University, Canberra, ACT 2601, Australia.
507 Farid Rahimi
508 Fondazione IRCCS Ca' Granda - Ospedale Maggiore Policlinico, Rare Diseases Center, Internal
509 Medicine Unit, Department of Medicine and Medical Specialties, Via Francesco Sforza, 35, 20122
510 Milan, Italy.
511 Elena Di Pierro and Giovanna Graziadei
512 School of Medicine, Deakin University, Warn Ponds, VIC 3216, Australia
513 Kathryn Matthews and Tania De Koning-Ward
514 Health and Biosecurity, CSIRO, Sydney, NSW 2113, Australia.
515 Denis C. Bauer

516

517

518 **Author Contributions**

519 CBS, HY, LS, AE, TKW, KM, FR, and BJM performed experiments and DCB analyzed the exome
520 sequencing data. The project was conceived by BJM, GB and SJF and experiments were designed by

521 CBS, HY, BJM and GB. The blood samples, and the genetic and biochemical analysis of the AIP
522 patients were provided and performed by EDP and GG. The paper was written and the figures were
523 prepared by CBS, EDP, GG, GB and BJM. All authors read and approved the final manuscript.
524
525 **Competing interests.**
526 The authors declare that they have no competing interests that might be perceived to influence the
527 results and/or discussion reported in this paper.
528
529 **Data Availability**
530 All data generated or analysed during this study are included in this article (and its Supplementary
531 Information files)
532
533 **Ethics approval and informed consent:**
534 Blood sampling and experimental procedures involving patients were performed in accordance with
535 the 1983 revision of the Declaration of Helsinki. The study was approved by the Ethical Committee
536 of Fondazione IRCCS Ca' Granda, Ospedale Maggiore Policlinico, Milan, Italy (Project Number
537 246_2015) and The Australian National University Human Research Ethics Committee (2014/765).
538 Written informed consent was obtained for each subject prior to study participation.
539 All procedures involving animals conformed to the *Australian code of practice for the care and use*
540 *of animals for scientific purposes* guidelines by the Australian National Health and Medical Research
541 Council and were approved by Macquarie University Animal Ethics Committee (Project Numbers:
542 ARA 2012/017 and 2012/019), the Australian National University Animal Experimentation Ethics
543 Committee (2014/53) and Deakin University animal ethics committee (Project Number G37-2013).
544
545

546 **REFERENCES**

547 [1] A.C. Allison, Genetic control of resistance to human malaria. Curr Opin Immunol 21 (2009)
548 499-505.
549 [2] A.V. Hill, The immunogenetics of resistance to malaria. Proc Assoc Am Physicians 111 (1999)
550 272-7.
551 [3] G. Min-Oo, and P. Gros, Erythrocyte variants and the nature of their malaria protective effect.
552 Cell Microbiol 7 (2005) 753-63.
553 [4] R.L. Nagel, and E.F. Roth, Jr., Malaria and red cell genetic defects. Blood 74 (1989) 1213-21.
554 [5] Z.Q. Bonday, S. Dhanasekaran, P.N. Rangarajan, and G. Padmanaban, Import of host delta-
555 aminolevulinate dehydratase into the malarial parasite: identification of a new drug target.
556 Nat Med 6 (2000) 898-903.
557 [6] S. Dhanasekaran, N.R. Chandra, B.K. Chandrasekhar Sagar, P.N. Rangarajan, and G.
558 Padmanaban, Delta-aminolevulinic acid dehydratase from Plasmodium falciparum:
559 indigenous versus imported. J Biol Chem 279 (2004) 6934-42.
560 [7] S. Koncarevic, P. Rohrbach, M. Deponte, G. Krohne, J.H. Prieto, J. Yates, 3rd, S. Rahlfs, and K.
561 Becker, The malarial parasite Plasmodium falciparum imports the human protein
562 peroxiredoxin 2 for peroxide detoxification. Proc Natl Acad Sci U S A 106 (2009) 13323-8.
563 [8] A. Sicard, J.P. Semblat, C. Doerig, R. Hamelin, M. Moniatte, D. Dorin-Semblat, J.A. Spicer, A.
564 Srivastava, S. Retzlaff, V. Heussler, A.P. Waters, and C. Doerig, Activation of a PAK-MEK
565 signalling pathway in malaria parasite-infected erythrocytes. Cell Microbiol 13 (2011) 836-
566 45.
567 [9] S. Varadharajan, B.K. Sagar, P.N. Rangarajan, and G. Padmanaban, Localization of
568 ferrochelatase in Plasmodium falciparum. Biochem J 384 (2004) 429-36.
569 [10] M. Brizuela, H.M. Huang, C. Smith, G. Burgio, S.J. Foote, and B.J. McMorran, Treatment of
570 erythrocytes with the 2-cys peroxiredoxin inhibitor, Conoidin A, prevents the growth of

571 Plasmodium falciparum and enhances parasite sensitivity to chloroquine. PLoS One 9
572 (2014) e92411.
573 [11] C.M. Smith, A. Jerkovic, T.T. Truong, S.J. Foote, J.S. McCarthy, and B.J. McMorran,
574 Griseofulvin impairs intraerythrocytic growth of Plasmodium falciparum through
575 ferrochelatase inhibition but lacks activity in an experimental human infection study. Sci
576 Rep 7 (2017) 41975.
577 [12] H. Ke, P.A. Sigala, K. Miura, J.M. Morrisey, M.W. Mather, J.R. Crowley, J.P. Henderson,
578 D.E. Goldberg, C.A. Long, and A.B. Vaidya, The heme biosynthesis pathway is essential
579 for Plasmodium falciparum development in mosquito stage but not in blood stages. J Biol
580 Chem 289 (2014) 34827-37.
581 [13] V.A. Nagaraj, B. Sundaram, N.M. Varadarajan, P.A. Subramani, D.M. Kalappa, S.K. Ghosh,
582 and G. Padmanaban, Malaria parasite-synthesized heme is essential in the mosquito and
583 liver stages and complements host heme in the blood stages of infection. PLoS Pathog 9
584 (2013) e1003522.
585 [14] Z. Rizopoulos, K. Matuschewski, and J.M. Haussig, Distinct Prominent Roles for Enzymes of
586 Plasmodium berghei Heme Biosynthesis in Sporozoite and Liver Stage Maturation. Infect
587 Immun 84 (2016) 3252-3262.
588 [15] P.A. Sigala, J.R. Crowley, J.P. Henderson, and D.E. Goldberg, Deconvoluting heme
589 biosynthesis to target blood-stage malaria parasites. Elife 4 (2015).
590 [16] Z.Q. Bonday, S. Taketani, P.D. Gupta, and G. Padmanaban, Heme biosynthesis by the malarial
591 parasite. Import of delta-aminolevulinate dehydrase from the host red cell. J Biol Chem 272
592 (1997) 21839-46.
593 [17] E.M. Pasini, M. Kirkegaard, P. Mortensen, H.U. Lutz, A.W. Thomas, and M. Mann, In-depth
594 analysis of the membrane and cytosolic proteome of red blood cells. Blood 108 (2006) 791-
595 801.

596 [18] E.M. Pasini, M. Kirkegaard, P. Mortensen, M. Mann, and A.W. Thomas, Deep-coverage
597 rhesus red blood cell proteome: a first comparison with the human and mouse red blood cell.
598 Blood Transfus 8 Suppl 3 (2010) s126-39.
599 [19] E.M. Pasini, M. Kirkegaard, D. Salerno, P. Mortensen, M. Mann, and A.W. Thomas, Deep
600 coverage mouse red blood cell proteome: a first comparison with the human red blood cell.
601 Mol Cell Proteomics 7 (2008) 1317-30.
602 [20] A. Brun, G. Gaudernack, and S. Sandberg, A new method for isolation of reticulocytes:
603 positive selection of human reticulocytes by immunomagnetic separation. Blood 76 (1990)
604 2397-403.
605 [21] C.M. Smith, A. Jerkovic, H. Puy, I. Winship, J.C. Deybach, L. Gouya, G. van Dooren, C.D.
606 Goodman, A. Sturm, H. Manceau, G.I. McFadden, P. David, O. Mercereau-Puijalon, G.
607 Burgio, B.J. McMorran, and S.J. Foote, Red cells from ferrochelatase-deficient
608 erythropoietic protoporphyria patients are resistant to growth of malarial parasites. Blood
609 125 (2015) 534-41.
610 [22] P.M. Lelliott, S. Lampkin, B.J. McMorran, S.J. Foote, and G. Burgio, A flow cytometric assay
611 to quantify invasion of red blood cells by rodent Plasmodium parasites in vivo. Malar J 13
612 (2014) 100.
613 [23] B.J. McMorran, V.M. Marshall, C. de Graaf, K.E. Drysdale, M. Shabbar, G.K. Smyth, J.E.
614 Corbin, W.S. Alexander, and S.J. Foote, Platelets kill intraerythrocytic malarial parasites
615 and mediate survival to infection. Science 323 (2009) 797-800.
616 [24] H. Puy, L. Gouya, and J.C. Deybach, Porphyrias. Lancet 375 (2010) 924-37.
617 [25] R.L. Lindberg, C. Porcher, B. Grandchamp, B. Ledermann, K. Burki, S. Brandner, A. Aguzzi,
618 and U.A. Meyer, Porphobilinogen deaminase deficiency in mice causes a neuropathy
619 resembling that of human hepatic porphyria. Nat Genet 12 (1996) 195-9.

620 [26] S. Clavero, D.F. Bishop, M.E. Haskins, U. Giger, R. Kauppinen, and R.J. Desnick, Feline
621 acute intermittent porphyria: a phenocopy masquerading as an erythropoietic porphyria due
622 to dominant and recessive hydroxymethylbilane synthase mutations. Hum Mol Genet 19
623 (2010) 584-96.
624 [27] K. Chen, J. Liu, S. Heck, J.A. Chasis, X. An, and N. Mohandas, Resolving the distinct stages
625 in erythroid differentiation based on dynamic changes in membrane protein expression
626 during erythropoiesis. Proc Natl Acad Sci U S A 106 (2009) 17413-8.
627 [28] D.C. Bauer, B.J. McMorran, S.J. Foote, and G. Burgio, Genome-wide analysis of chemically
628 induced mutations in mouse in phenotype-driven screens. BMC Genomics 16 (2015) 866.
629 [29] H. Li, and R. Durbin, Fast and accurate short read alignment with Burrows-Wheeler transform.
630 Bioinformatics 25 (2009) 1754-60.
631 [30] B. Langmead, and S.L. Salzberg, Fast gapped-read alignment with Bowtie 2. Nat Methods 9
632 (2012) 357-9.
633 [31] H. Li, B. Handsaker, A. Wysoker, T. Fennell, J. Ruan, N. Homer, G. Marth, G. Abecasis, R.
634 Durbin, and S. Genome Project Data Processing, The Sequence Alignment/Map format and
635 SAMtools. Bioinformatics 25 (2009) 2078-9.
636 [32] A. McKenna, M. Hanna, E. Banks, A. Sivachenko, K. Cibulskis, A. Kernytsky, K. Garimella,
637 D. Altshuler, S. Gabriel, M. Daly, and M.A. DePristo, The Genome Analysis Toolkit: a
638 MapReduce framework for analyzing next-generation DNA sequencing data. Genome Res
639 20 (2010) 1297-303.
640 [33] K. Wang, M. Li, and H. Hakonarson, ANNOVAR: functional annotation of genetic variants
641 from high-throughput sequencing data. Nucleic Acids Res 38 (2010) e164.
642 [34] C.M. Benton, C.K. Lim, C. Moniz, and D.J. Jones, Ultra high-performance liquid
643 chromatography of porphyrins in clinical materials: column and mobile phase selection and
644 optimisation. Biomedical chromatography : BMC 26 (2012) 714-9.

645 [35] C.M. Benton, C.K. Lim, H.J. Ritchie, C. Moniz, and D.J. Jones, Ultra high-performance liquid
646 chromatography of porphyrins. Biomedical chromatography : BMC 26 (2012) 331-7.
647 [36] E.J. Erlandsen, P.E. Jorgensen, S. Markussen, and A. Brock, Determination of porphobilinogen
648 deaminase activity in human erythrocytes: pertinent factors in obtaining optimal conditions
649 for measurements. Scand J Clin Lab Invest 60 (2000) 627-34.
650 [37] W. Trager, and J.B. Jensen, Human malaria parasites in continuous culture. Science 193 (1976)
651 673-5.
652 [38] E.M. Rivadeneira, M. Wasserman, and C.T. Espinal, Separation and concentration of schizonts
653 of Plasmodium falciparum by Percoll gradients. J Protozool 30 (1983) 367-70.
654 [39] U.K. Laemmli, Cleavage of structural proteins during the assembly of the head of
655 bacteriophage T4. Nature 227 (1970) 680-5.
656 [40] S. Haase, E. Hanssen, K. Matthews, M. Kalanon, and T.F. de Koning-Ward, The exported
657 protein PbCP1 localises to cleft-like structures in the rodent malaria parasite Plasmodium
658 berghei. PloS one 8 (2013) e61482.
659 [41] C.J. Janse, J. Ramesar, and A.P. Waters, High-efficiency transfection and drug selection of
660 genetically transformed blood stages of the rodent malaria parasite Plasmodium berghei.
661 Nature protocols 1 (2006) 346-56.
662 [42] C.J. Janse, B. Franke-Fayard, G.R. Mair, J. Ramesar, C. Thiel, S. Engelmann, K.
663 Matuschewski, G.J. van Gemert, R.W. Sauerwein, and A.P. Waters, High efficiency
664 transfection of Plasmodium berghei facilitates novel selection procedures. Mol Biochem
665 Parasitol 145 (2006) 60-70.
666
667
668
669
670

671 **FIGURE LEGENDS:**

672

673 **Figure 1. Analysis of the *Pbgd*^{MRI58155} mutation.**

674 **(A)** Schematic of the full-length 361 residue murine PBGD protein, including locations of the three
675 domains and active site residues, R^{25} and S^{28} (sulfate-binding), D^{99} (catalytic), S^{147}, R^{150} and R^{173}
676 (pyrrole-cofactor-interacting) and C^{261} (pyrrole-cofactor-binding), based on a solved human PBGD
677 crystal structure; Gill et al 2009). The predicted 90 residue PBGD^{MRI58155} protein is shown below. Its
678 lacks the sequences containing the catalytic domain and cofactor binding sites. (**B**) Measurement of
679 PBGD enzyme activity in whole blood samples from WT and Het mice using HPLC. Data represent
680 the mean (box) and values from four mice per group, each assayed two times. * $p < 0.05$, calculated
681 using a two-tailed *t*-test assuming equal variance.

682

683 **Figure 2: Mice with the *Pbgd*^{MRI58155} mutation display an increased resistance to infection with**
684 ***P. chabaudi*.**

685 **(A and B)** Parasite growth and **(C and D)** survival in *Pbgd*^{MRI58155} heterozygotes (Het) and wild-type
686 littermates (WT) infected with *P. chabaudi* ($1x10^4$ parasites; 13-21 mice per group). **(E)** Parasitemia
687 measured at various timepoints in labeled donor RBC following transfusion into *P. chabaudi* infected
688 recipient mice (eight days after parasite inoculation). Donor RBC were from *Pbgd*^{MRI58155}
689 heterozygotes (Het) or wild-type littermates (WT) (8 recipient mice per group). **(F)** Proportions of
690 TUNEL-labeled parasite-infected erythrocytes in *Pbgd*^{MRI58155} heterozygotes (Het) or wild-type
691 littermates (WT) infected with *P. chabaudi* (five per group). Error bars represent SEM. * $p < 0.05$,
692 ** $p < 0.01$, calculated using a two-tailed *t*-test assuming equal variance. Log-rank (Mantel-Cox test)
693 for differences in survival yielded $p = 0.0016$ (female group) and $p = 0.16$ (male).

694

695 **Figure 3. Parasite growth analysis of wild-type and *Pbgd*-knockout *P. berghei* in wild-type and**
696 ***Pbgd*$^{MRI58155/+}$ deficient mice.**

697 Blood parasitemia determined in WT and *Pbgd*^{MRI58155} heterozygous (Het) mice after infection with
698 either *Pbgd*-knockout *P. berghei* (*PbA_Pbgd* KO) or parental wild-type (WT). For parasite lines the
699 starting inoculum was 1x104 parasites. The data represent the mean (+/- SD) for 8 to 15 mice per
700 group. Data per group). growth in infected WT and *Pbgd*^{MRI58155} heterozygous mice. There were no
701 statistically significant differences comparing the four different parasite and animal combinations on
702 each day of the infection using two-way ANOVA.
703
704 **Figure 4. Parasite growth analysis of wild-type and *Pbgd*-knockout *P. falciparum* in**
705 **erythrocytes from normal and AIP individuals.**
706 Parasite growth following inoculation of wild-type (*Pbgd* WT) or *Pbgd*-knockout (*Pbgd* KO) *P.*
707 *falciparum* into erythrocytes isolated from healthy individuals (Normal ARC and Normal Italy) and
708 from four AIP individuals (A-D; see Table S4 for biochemical and PBGD activity characteristics).
709 The parasites were cultured for up to 72 h. Data represent the mean fold changes (+- SD) for two
710 independent growth assay experiments, except for AIP B which was assayed once. There were no
711 statistically significant differences comparing between the Normal and AIP samples, or between the
712 two parasite strains using two-way ANOVA.
713
714 **SUPPLEMENTAL FIGURE LEGENDS**

715 **Figure S1: Hematological analysis of the *Pbgd*^{MRI58155} mouse line.**
716 **(A)** Comparison of erythrocyte life span, (**B)** osmotic strength, and (**C)** bone-marrow erythroid
717 progenitor cells in *Pbgd*^{MRI58155} heterozygotes (Het, n = six to nine mice) and wild-type littermates
718 (WT, n = six to seven mice). Error bars represent SEM. No significant differences were observed
719 between groups using the two-tailed Student's *t*-test assuming equal variance.

720 **Figure S2: Generation of *Pbgd P. berghei* knockout.**

721 **(A)** For targeted gene deletion of the PbANKA_060800, fragments of the 5' UTR and 3' UTR,
722 which would serve as targeting regions to drive integration into the endogenous locus, were PCR-
723 amplified from *P. berghei* ANKA genomic DNA and cloned into the p35/EF5'.Fluc.CAM3' vector.
724 Position of oligonucleotides used for PCR analysis are shown. (**B)** Representation of a gel
725 electrophoresis on the genomic integration of the targeting construct using specific primers
726 spanning the locus. SM, *hDHFR* selectable marker; I, integrant fragment size; E, non- integrant
727 fragment size.

Figure 1

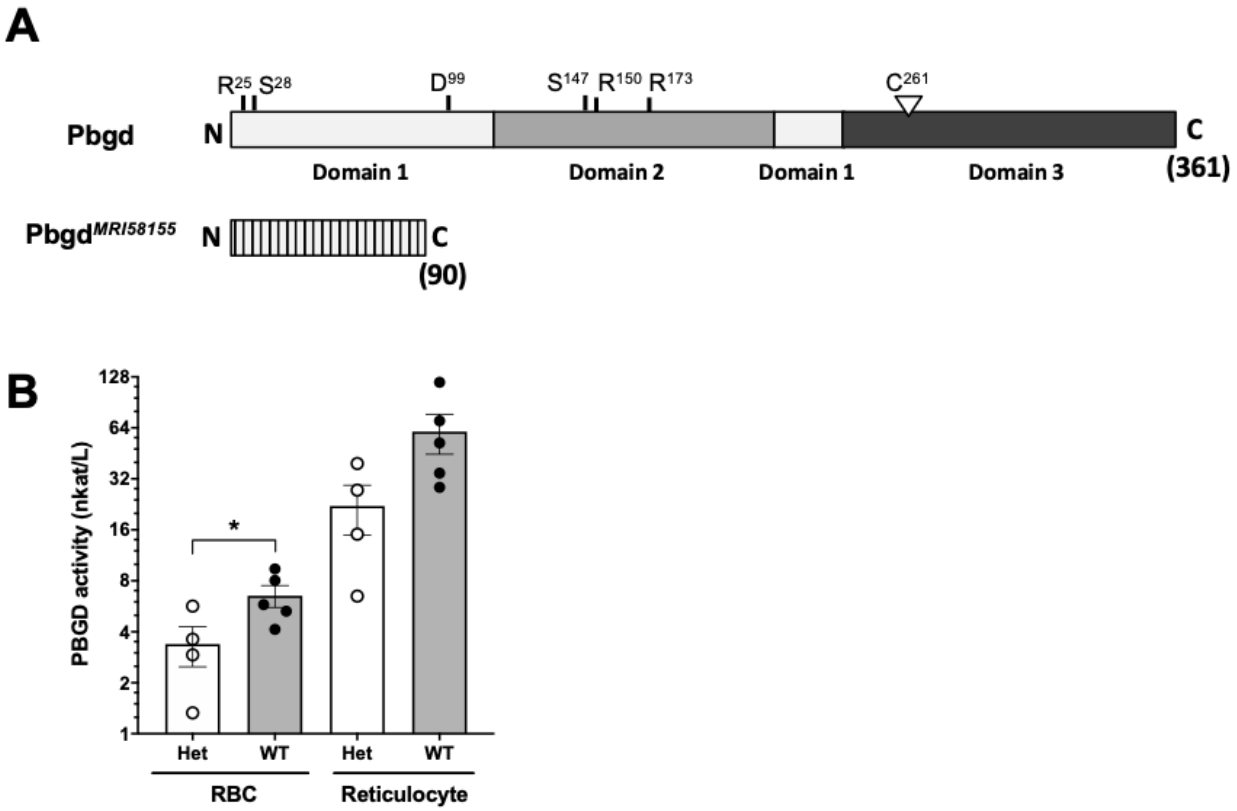
A
R25 S28
D99
S147 R150 R173
C261
Pbgd
N
C
(361)
Domain 1
Domain 2
Domain 1
Domain 3
Pbgd MRI58155
N
C
(90)
B
PBGD activity (nkat/L)
128
64
32
16
8
4
2
1
*
Het
WT
Het
WT
RBC
Reticulocyte

Figure 2

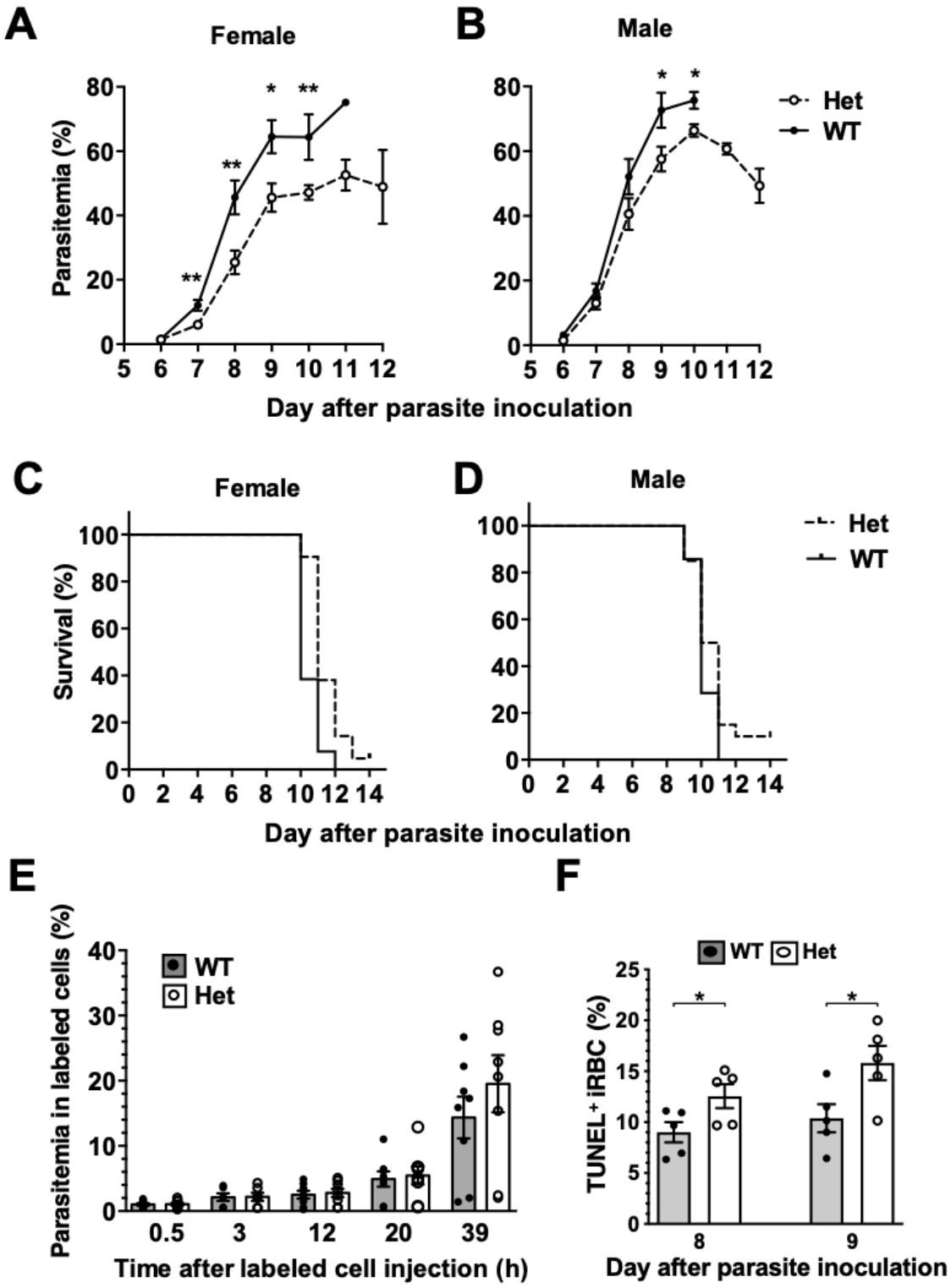
A
Female
Parasitemia (%)
80
60
40
20
0
5 6 7 8 9 10 11 12
**
**
*
**
B
Male
*
*
Het
WT
Day after parasite inoculation
C
Female
Survival (%)
100
80
60
40
20
0
0 2 4 6 8 10 12 14
D
Male
Het
WT
Day after parasite inoculation
E
Parasitemia in labeled cells (%)
40
30
20
10
0
WT
Het
0.5
3
12
20
39
Time after labeled cell injection (h)
F
WT
Het
TUNEL+ iRBC (%)
25
20
15
10
5
0
*
*
8
9
Day after parasite inoculation

Figure 3

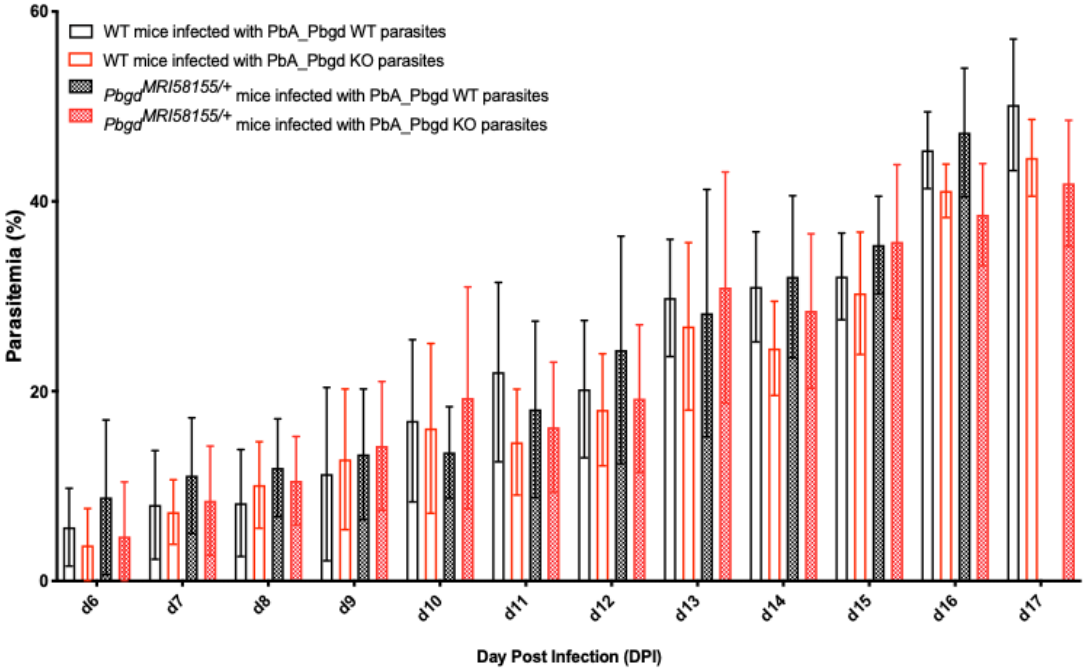
WT mice infected with PbA_Pbgd WT parasites
WT mice infected with PbA_Pbgd KO parasites
PbgdMRI58155/+ mice infected with PbA_Pbgd WT parasites
PbgdMRI58155/+ mice infected with PbA_Pbgd KO parasites
Parasitemia (%)
60
40
20
0
d6
d7
d8
d9
d10
d11
d12
d13
d14
d15
d16
d17
Day Post Infection (DPI)

Figure 4

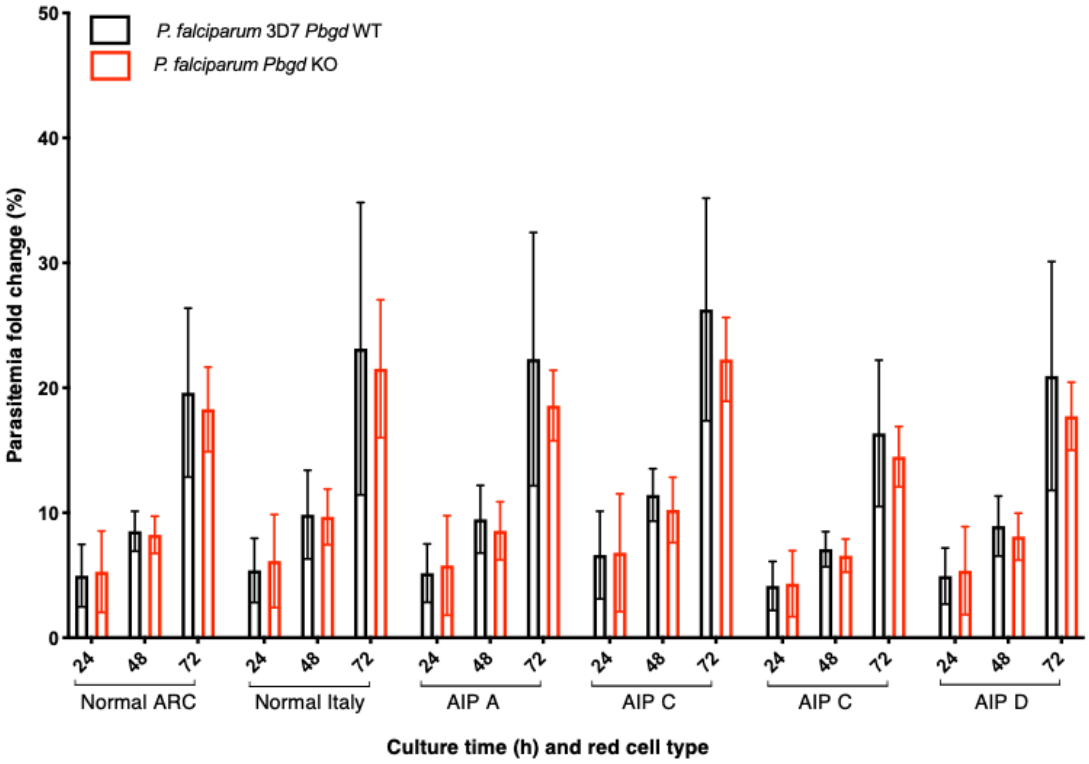
P. falciparum 3D7 Pbgd WT
P. falciparum Pbgd KO
Parasitemia fold change (%)
50
40
30
20
10
0
24
48
72
Normal ARC
Normal Italy
AIP A
AIP C
AIP C
AIP D
Culture time (h) and red cell type

Figure S1

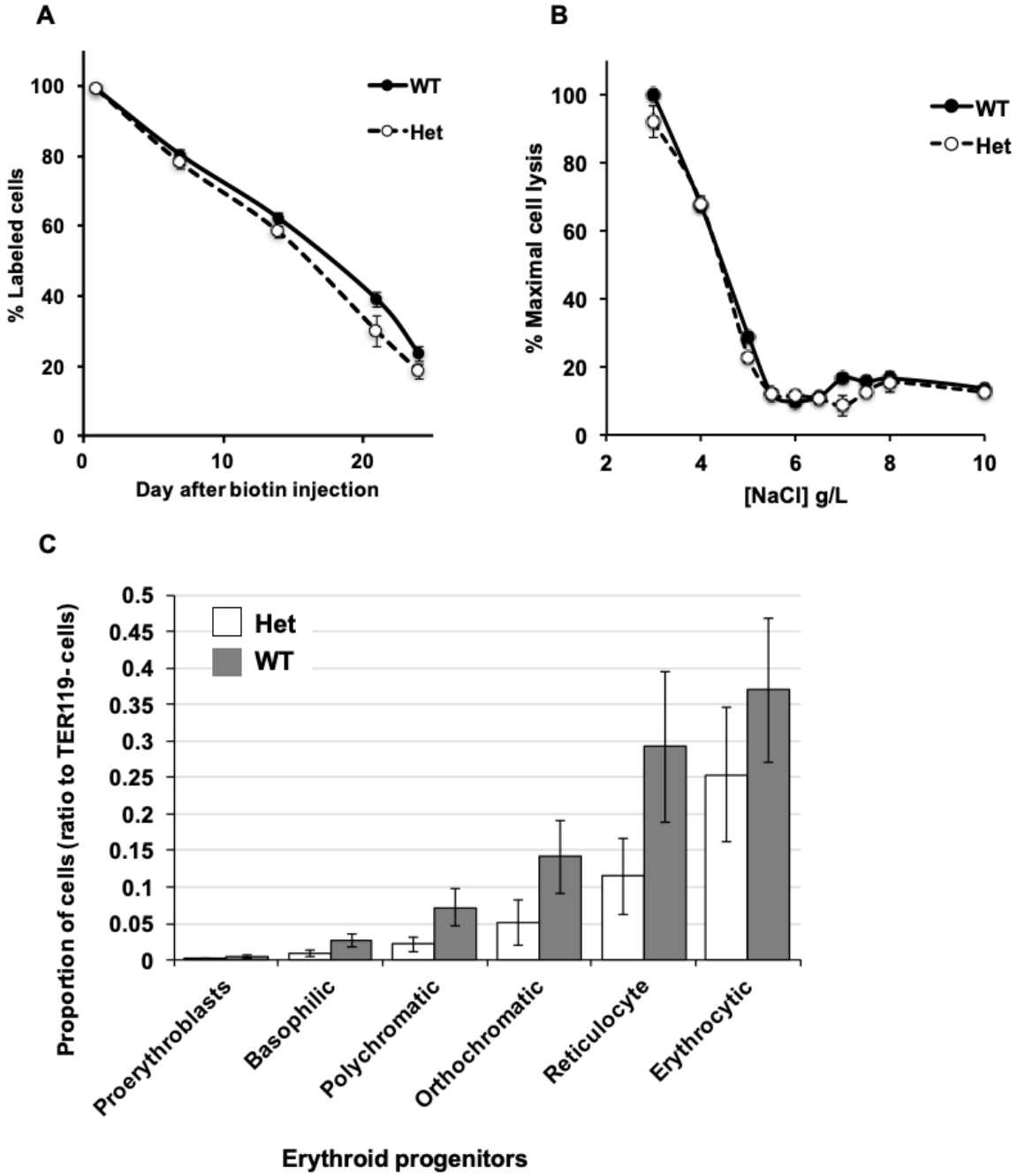
A
% Labeled cells
Day after biotin injection
WT
Het
B
% Maximal cell lysis
[NaCl] g/L
WT
Het
C
Proportion of cells (ratio to TER119- cells)
Het
WT
Proerythroblasts
Basophilic
Polychromatic
Orthochromatic
Reticulocyte
Erythrocytic
Erythroid progenitors

Figure S2

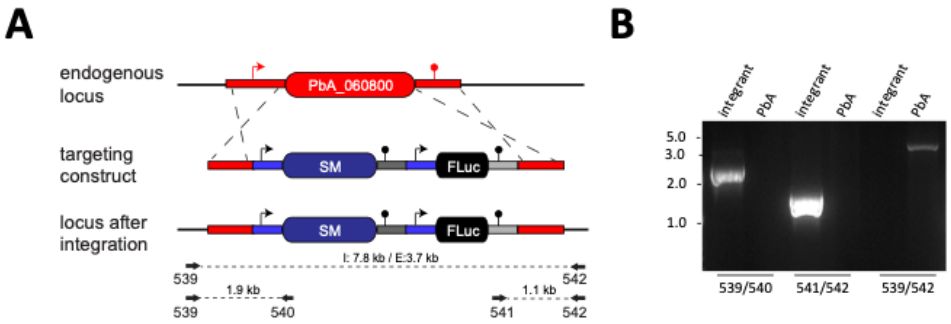
A
endogenous locus
PbA_060800
targeting construct
SM
FLuc
locus after integration
SM
FLuc
I: 7.8 kb / E:3.7 kb
539
542
1.9 kb
539
540
1.1 kb
541
542
B
Integrant
PbA
Integrant
PbA
Integrant
PbA
5.0
3.0
2.0
1.0
539/540
541/542
539/542

SUPPLEMENTAL TABLES

Table S1. Hematological parameters of wild-type and *Pbgd*^{MRI58155} heterozygous mice. Automated full blood analysis on SJL mice (n = 500), wild type (n = 24) and heterozygous (n = 63) mice. RBC = erythrocyte; WBC = white blood cell; MCV = mean corpuscular volume; HCT = haematocrit; % retics = proportion of reticulocytes; HGB = hemoglobin concentration; MCHC = mean corpuscular hemoglobin concentration. Values denote mean ± SEM. ** $p < 0.01$; *** $p < 0.001$.

	RBC	WBC	MCV	HCT	Retics (%)	HGB (g/L)	MCHC (g/L)
Het	10.11 ± 0.17	11.09 ± 0.38	49.95 ± 0.22***	0.50 ± 0.008***	5.84 ± 0.26***	141.8 ± 2.5***	215.5 ± 7.4
WT	10.25 ± 0.05	11.44 ± 0.45	52.40 ± 0.23	0.54 ± 0.003	3.24 ± 0.21	153.4 ± 0.8	210 ± 6.5
SJL/J	9.79 ± 0.22	11.84 ± 0.50	52.61 ± 0.19	0.51 ± 0.011	3.44 ± 0.033	153.84 ± 0.23	203.53 ± 7.95

Table S2. Spleen and liver indices, and non-heme iron content in wild-type and *Pbgd*^{MRI58155} heterozygous mice (n = 3 per group). Values denote means ± SD. * $p < 0.05$.

	Spleen index	Liver index	Spleen iron (mg/g)	Liver iron (mg/g)
Het	0.477 ± 0.017*	5.8 ± 0.33	15.2 ± 1.2	3.59 ± 0.65
WT	0.408 ± 0.009	5.96 ± 0.16	11.4 ± 0.2	4.58 ± 0.62

Table S3. Serum cytokine concentrations in wild-type (n = 5) and *Pbgd*^{MRI58155} heterozygous (n = 8) mice. All cytokine concentrations are pg/mL plasma. Values denote means ± SD. * $p < 0.05$.

	IL-2	IL-4	IL-6	IFNγ	TNFα	IL-10	IL-17A
Het	119 ± 55	122 ± 56	84 ± 54	68 ± 42	140 ± 85	93 ± 42*	110 ± 51*
WT	192 ± 51	157 ± 56	156 ± 87	111 ± 53	186 ± 92	146 ± 34	187 ± 53

18 **Table S4. AIP patient blood biochemistry.** * Patients were symptomatic for AIP at the time of

19 blood collection.

AIP patient ID	ALA/Creatinine ratio	PBG/Creatinine ratio	Total urinary porphyrins (µg/L)	% Urine porphyrin types (URO, EPTA, ESA, PENTA, COPRO I, COPRO III)	PBGD activity (pmol/h/mg Hb)
A	2.3	0.4	73	4, 1, <1, 10, 37, 48	61.1
B*	18.6	11.1	179	43, 3, 3, 22, 17, 12	74.8
C*	24.4	3.4	575	24, 2, 3, 23, 8, 41	56.9
D	1.5	0.3	88	8, 4, 1, 8, 58, 21	57.5

20

21

22

23